Effect of Temperature and Pressure on Surface Tension of Polystyrene in Supercritical Carbon Dioxide

H. Park[1], R.B. Thompson[2], N. Lanson[3] C. Tzoganakis[1], C.B. Park[4], and P. Chen[1,]*

Departments of [1]Chemical Engineering, [2]Physics and Astronomy, and [3]Applied Mathematics

University of Waterloo, 200 University Avenue,

Waterloo, Ontario, Canada N2L 3G1

[4]Microcellular Plastics Manufacturing Laboratory, Department of Mechanical and Industrial Engineering, University of Toronto, 5 King's College Road,

Toronto, Ontario, Canada M5S 3G8

* Corresponding author: p4chen@uwaterloo.ca

Abstract

The surface tension of polymers in a supercritical fluid is one of the most important physicochemical parameters in many engineering processes, such as microcellular foaming where the surface tension between a polymer melt and a fluid is a principal factor in determining cell nucleation and growth. This paper presents experimental results of the surface tension of polystyrene in supercritical carbon dioxide, together with theoretical calculations for a corresponding system. The surface tension is determined by Axisymmetric Drop Shape Analysis-Profile (ADSA-P), where a high pressure and temperature cell is designed and constructed to facilitate the formation of a pendant drop of polystyrene melt. Self-consistent field theory (SCFT) calculations are applied to simulate the surface tension of a corresponding system, and good qualitative agreement with experiment is obtained. The physical mechanisms for three main experimental trends are explained using SCFT, and none of the explanations quantitatively depend on the configurational entropy of the polymer constituents. These calculations therefore rationalize the use of simple liquid models for the quantitative prediction of surface tensions of polymers. As pressure and temperature increase, the surface tension of polystyrene decreases. A linear relationship is found between surface tension and temperature, and between surface tension and pressure; the slope of surface tension change with temperature is dependent on pressure.

Introduction

Surface tension is one of the most important physicochemical properties for polymeric materials in various engineering processes, such as those involving foaming, suspensions, wetting and blending [1]. In the foaming of polymer melts, the homogeneous nucleation rate is described by $N_{\text{homo}}^{\text{o}} = C_o f_o \exp(-\Delta G_{\text{homo}} / k_B T)$ according to bubble nucleation theories, where $N_{\text{homo}}^{\text{o}}$ is the number of nuclei generated per cm^3 per second, C_o the concentration of gas molecules (number of molecules per cm^3), f_o the frequency factor of the gas molecules, ΔG_{homo} the Gibbs free energy for homogeneous nucleation, and k_B Boltzmann's constant [2, 3]. The Gibbs free energy (ΔG_{homo}) for homogeneous nucleation is given by $\Delta G_{\text{homo}} = 16\pi\gamma^3 / 3\Delta P^2$, where γ is the surface tension between the polymer phase and nucleating bubble phase, and ΔP the pressure difference between the metastable solution and a hypothetical nucleated phase of pure gas at the same temperature and chemical potential. When the polymer in carbon dioxide has a lower surface tension than that of the pure polymer, the Gibbs free energy will be reduced by the cubic power of the surface tension, and the nucleation rate will increase exponentially. It is evident that changes in surface tension are crucial to polymer foaming processes, and it is necessary to understand and control such a property in order to optimize such polymer-involved industrial operations [4, 5].

There are many methods to measure surface tension. Among them, the pendant drop method has many advantages because of simplicity and versatility in its setup and principle [6, 7]. The pendant drop method has been used extensively for low molar mass liquids, liquid crystals and polymers. This method relies on the determination of a drop profile of dense liquid in another fluid, and the surface tension of the liquid is obtained from the best fit of the Laplace equation of

capillarity to the experimentally determined drop profile [8, 9]. Although the pendant drop method is theoretically simple, the research to date for determining surface tension of polymers has been limited because of experimental difficulties in handling high viscosity polymer melts under high temperature and high pressure [10, 11, 12]. In fact, there have been only limited surface tension data available for a few select polymers, and the range of experimental conditions, to which polymers are subjected during their measurements, has been rather narrow. All of these shortcomings make the understanding and control of the surface tension of polymers difficult.

Supercritical carbon dioxide has been used as a foaming agent in the production of microcellular polymer foams [13, 14]. Carbon dioxide has main advantages of being non-toxic and having a relatively low critical point (T_c=31C, P_c=7.376 MPa or 1070 psi). Although small amounts of carbon dioxide are added to the polymer process, dramatic changes result in physicochemical properties, such as glass transition temperature, viscosity, solubility and surface tension [15]. Particularly, the surface tension between polymer and gas phases has been emphasized because it significantly affects the foaming and morphology of final polymer products.

The primary objective of this study is to quantify the surface tension of a typical, commercially available polymer, polystyrene, in supercritical carbon dioxide, and to understand its dependence on temperature and pressure in a systematic way. A recently designed high-temperature and high-pressure sample cell is employed in the surface tension measurement to achieve a wide range of experimental conditions. With the collection of a comprehensive set of surface tension data, an empirical equation to approximate the surface tension of polystyrene in supercritical carbon dioxide as a function of temperature and pressure is developed, which provides predictive

power for the surface tension variation. Furthermore, trends of the surface tension change with temperature and pressure are elucidated, and in particular, the effect of temperature on surface tension is shown to depend on the value of pressure.

To understand the surface tension behavior further, theoretical analysis of the experimental trends is given using self-consistent field theory (SCFT). It is difficult to achieve numerical accuracy for realistic values of the present system, so only qualitative agreement is sought. In this context, agreement with experiment is found, and three surface tension trends involving temperature and pressure are explained in terms of components of the surface tension. These components can be related to molecular interactions and configurations of polymers and, to some extent, solvents (CO_2 in the present case). The resulting information provides means to change/ control the surface tension during polymer processing, through chemical and composition design of polymer materials. Specifically, it is found that a reduction in surface tension with increasing temperature is due to an expected increased mixing of chemical constituents upon reducing the segregation parameters between dissimilar constituents (polystyrene and supercritical carbon dioxide) with increasing temperature. A decrease in surface tension with increasing pressure is, however, due to more similar densities between these dissimilar constituents. Related to this, it is found that the slope of surface tension with temperature itself decreases at higher pressures. SCFT shows this to be due to increased mixing between dissimilar constituents at higher pressure that results from the increased similarity in density. None of these explanations for the experimental trends are found to depend qualitatively on the configurational entropy contribution to the surface tension of the polymer, so these calculations rationalize the use of simple liquid models [16, 17] for the quantitative prediction of surface tensions of polymers.

Experimental

Materials

Polystyrene used was a commercial product (Styron 685D, Mn =120,000, polydispersity index=2.6) from Dow Chemical Company. Carbon dioxide used was of chromatographic grade (purity of 99.99%), purchased from PRAXAIR, Danbury, CT, USA.

Surface tension measurement

The surface tension of polystyrene in carbon dioxide was measured at temperatures from 170 to 210°C, within a wide range of pressures, from 500 to 2500 psi. To achieve these experimental conditions, a high-temperature and high-pressure sample cell was constructed. Briefly, this optical viewing cell consisted of a cylinder of stainless steel, which was heated by an electrical heater. The inside of the cylinder was hollow, with a diameter of 30 mm and length of 25 mm. Two optical-quality sapphire windows (Meller Optics, Inc.) permitted the illumination and observation of the pendant drop formed by a sample polymer melt. The setup was tested for its accuracy and reproducibility with a range of polymer-gas combinations, and the details of this were described in a recent publication [18].

The technique of Axisymmetric Drop Shape Analysis-Profile(ADSA-P) [19, 20] was used for image analysis and parameter extraction. Surface or interfacial tensions were obtained by fitting the Laplace equation of capillarity to the shape and dimensions of axisymmetric menisci acquired [21]. The value of surface tension was generated as a fitting parameter [22] after a least square algorithm was employed to minimize the difference between experimental drop profiles

and theoretical ones. During this procedure, the density difference between polystyrene and carbon dioxide was an input parameter [23, 24, 25], which was determined by the Sanchez and Lacombe (S-L) equation of state (EOS) [26-29], see Supporting Information.

Theory

To understand the surface tension and its dependence on temperature and pressure, experimentally determined surface tensions can be compared to surface tensions calculated using self-consistent field theory (SCFT). SCFT is an equilibrium statistical mechanical approach for determining structures in polymeric systems. It is based on a free energy functional, which is to be minimized in order to find the lowest energy morphology. The procedure for deriving such functionals is explained in depth in a number of reviews [30-33]. For the supercritical carbon dioxide-polystyrene system, the appropriate free energy functional can be derived in the canonical ensemble to be

$$\begin{aligned}\frac{NF}{\rho_0 k_B T V} = &-\frac{\phi_s}{\alpha}\ln\left(\frac{Q_s\alpha}{V\phi_s}\right)-\frac{\phi_h}{\alpha}\ln\left(\frac{Q_h\alpha}{V\phi_h}\right)-\phi_p\ln\left(\frac{Q_p}{V\phi_p}\right)\\ &+\frac{1}{V}\int d\mathbf{r}\{\chi_{ps}N\varphi_p(\mathbf{r})\varphi_s(\mathbf{r})+\frac{1}{2}\chi_{ss}N\varphi_s(\mathbf{r})\varphi_s(\mathbf{r})+\frac{1}{2}\chi_{pp}N\varphi_p(\mathbf{r})\varphi_p(\mathbf{r})\\ &-\omega_s(\mathbf{r})\varphi_s(\mathbf{r})-\omega_h(\mathbf{r})\varphi_h(\mathbf{r})-\omega_p(\mathbf{r})\varphi_p(\rho)\\ &-\xi(\mathbf{r})[1-\varphi_s(\mathbf{r})-\varphi_p(\mathbf{r})-\varphi_h(\mathbf{r})]\}\end{aligned} \quad (1)$$

where F/V is the free energy of the system per volume V. This free energy is made dimensionless by dividing by k_BT and multiplying by the volume of a single polymer N/ρ_0, where $1/\rho_0$ is the volume of a single polymer segment and N is the degree of polymerization based on that segment volume. It should be noted that since SCFT is a coarse-grained theory, a

single segment may include many chemical monomers. On the right hand side of (1), ϕ_s, ϕ_p, and ϕ_h are the overall volume fractions of solvent molecules, polymer segments and "holes", respectively. In order to be consistent with the Sanchez-Lacombe equation of state [27] being used experimentally to extract the surface tension, we are also using a Sanchez-Lacombe equation of state to model pressure in the SCFT. This approach was introduced by Hong and Noolandi [34] for SCFT and consists of treating a compressible system as an incompressible system together with vacancies, that is, holes. Higher pressure systems have fewer holes whereas lower pressure systems have more. The Sanchez-Lacombe equation of state thus relates the density to pressure for systems whose variable density is modeled in terms of holes. With this in mind, the volume fractions ϕ_s, ϕ_p, and ϕ_h are not all independent, rather $\phi_s+\phi_p+\phi_h=1$. It should be noted that other approaches for treating compressibility within SCFT are possible, in particular Binder *et al*. have studied solvent-polymer systems thoroughly using a virial expansion to get an equation of state [35]. The local volume fractions of solvent, polymer and holes are given by $\varphi_s(\mathbf{r})$, $\varphi_p(\mathbf{r})$, and $\varphi_h(\mathbf{r})$, respectively, in equation (1). Conjugate to these are the position dependent chemical potential fields $\omega_s(\mathbf{r})$, $\omega_p(\mathbf{r})$ and $\omega_h(\mathbf{r})$, and a pressure field $\xi(\mathbf{r})$ which enforces incompressibility with respect to *all* the chemical species: solvent, polymer and holes. The physical pressure can then be found, if desired, by calculating the appropriate osmotic pressure within the formalism. The Flory-Huggins parameters are usually defined in terms of dissimilar constituents such as χ_{ps}, χ_{ph} and χ_{sh}. It is felt here however that since the holes are fictitious, it is more meaningful to choose our three independent parameters as χ_{ps}, χ_{pp} and χ_{ss}. They are defined from first principles as

$$\chi_{ij} = \frac{\rho_0}{k_B T}\int d\mathbf{r} V_{ij}(|\mathbf{r}|) \tag{2}$$

where $V_{ij}(|\mathbf{r}|)$ is two-body potential between species i and j with $i, j = p, s$ or h [34]. Since the potential between holes and anything else should be zero, all χ terms in the free energy involving h will vanish. The interpretation of these parameters is then no longer as the dimensionless change in energy upon exchange of segments between pure components, although the use of the term Flory-Huggins parameter will be maintained; they still arise as the first order in a gradient expansion of the potentials [36].

Usually, the products (χN) are taken as the segregation parameters instead of just the parameter(χ). The ratio of the volume of a solvent molecule to a polymer molecule is given by α. Finally, Q_s, Q_p and Q_h are the partition functions for single molecules of solvent, polymer and holes, respectively, subject to the fields $\omega_s(\mathbf{r})$, $\omega_p(\mathbf{r})$ and $\omega_h(\mathbf{r})$. Expressions for these partition functions are given below in equations (10), (11), and (12). The variation of (1) with respect to the functions $\varphi_s(\mathbf{r})$, $\varphi_p(\mathbf{r})$, $\varphi_h(\mathbf{r})$, $\omega_s(\mathbf{r})$, $\omega_p(\mathbf{r})$, $\omega_h(\mathbf{r})$ and $\xi(\mathbf{r})$ results in a set of equations for these functions that must be solved self-consistently, and usually, numerically. The equations are

$$\omega_s(\mathbf{r}) = \chi_{ps} N\varphi_p(\mathbf{r}) + \chi_{ss} N\varphi_s(\mathbf{r}) + \xi(\mathbf{r}) \tag{3}$$

$$\omega_p(\mathbf{r}) = \chi_{ps} N\varphi_s(\mathbf{r}) + \chi_{pp} N\varphi_p(\mathbf{r}) + \xi(\mathbf{r}) \tag{4}$$

$$\omega_h(\mathbf{r}) = \xi(\mathbf{r}) \tag{5}$$

$$\varphi_s(\mathbf{r}) + \varphi_p(\mathbf{r}) + \varphi_h(\mathbf{r}) = 1 \tag{6}$$

$$\varphi_s(\mathbf{r}) = \frac{\phi_s V}{Q_s} e^{-\alpha\omega_s(\mathbf{r})} \tag{7}$$

$$\varphi_h(\mathbf{r}) = \frac{\phi_h V}{Q_h} e^{-\alpha\omega_h(\mathbf{r})} \tag{8}$$

$$\varphi_p(\mathbf{r}) = \frac{\phi_p V}{Q_p} \int_0^1 ds q(\mathbf{r}, s) q(\mathbf{r}, 1-s) \tag{9}$$

with

$$Q_s = \int d\mathbf{r} e^{-\alpha\omega_s(\mathbf{r})} \tag{10}$$

$$Q_h = \int d\mathbf{r} e^{-\alpha\omega_h(\mathbf{r})} \tag{11}$$

$$Q_p = \int d\mathbf{r} q(\mathbf{r}, 1) \tag{12}$$

and

$$\frac{\partial q(\mathbf{r}, s)}{\partial s} = \frac{Na^2}{6} \nabla^2 q(\mathbf{r}, s) - \omega_p(\mathbf{r}) q(\mathbf{r}, s) \tag{13}$$

In (13), a is the "statistical segment length" of a polymer segment; the definition of a and more details about SCFT can be found in references [30-33].

The equations (3)-(13) are solved numerically in real space, using a Crank-Nicolson algorithm with reflecting boundary conditions (requiring derivatives of spatially dependent functions to be zero at the boundaries) in one dimension in order to find the structure and free energy of the interfacial system. A random initial guess for the fields is taken, the diffusion equations are solved and the local volume fractions found. Also from this guess, the incompressibility constraint is calculated. The local volume fractions together with the incompressibility constraint allow new fields to be computed. This process is iterated until the new fields and the old fields differ by less than one part in 10^{-11} according to the criteria of [37]. The independent input parameters for this process are α, $\chi_{ps}N$, $\chi_{pp}N$ and, $\chi_{ss}N$. The volume V (or L in one dimension) is arbitrary, provided it is taken large enough such that the system

reaches bulk conditions on either side of the interface. Similarly, ϕ_s and ϕ_p can take a range of values provided there is enough total polymer and solvent present for bulk conditions to be reached. Varying the amount of ϕ_s or ϕ_p within reason simply shifts the interface in one direction or the other within the calculational region L. Therefore there are only four important parameters for the model system, although we shall continue specifying the ϕ_s and ϕ_p used in any given calculation for clarity.

Upon obtaining solutions for (3)-(13), the free energy for the system can be found through (1). The surface tension γ may then be calculated through a generalization of the binary surface tension formula given by Matsen [30]. In dimensionless form, we write this as

$$\frac{R_g \gamma}{a^2 \rho_0 k_B T} = \left(\frac{L}{R_g} \right) \left(\frac{NF}{\rho_0 k_B T V} - \sum_{i=p,s,h} \frac{NF_{si}}{\rho_0 k_B T V} \right) \tag{14}$$

where the unperturbed radius of gyration of a polymer $R_g = aN^{1/2}/\sqrt{6}$ is used as the length scale in all our SCFT calculations. In (14), we are essentially subtracting off the free energy of the bulk phases on either side of the interface to leave the energy of the interface itself; this is then phrased as a surface tension by dividing by the interfacial area. The free energy of the bulk phases is given by $\sum_{i=p,s,h} \frac{NF_{si}}{\rho_o k_B T V}$, where each of the F_{si} terms is defined as

$$\frac{NF_{si}}{\rho_0 k_B T V} = \frac{NF_{hi}^{(1)}}{\rho_0 k_B T V} \left(\frac{V_{1i}}{V} \right) + \frac{NF_{hi}^{(2)}}{\rho_0 k_B T V} \left(1 - \frac{V_{1i}}{V} \right) \tag{15}$$

with $F_{hi}^{(1)}$ and $F_{hi}^{(2)}$ corresponding to the free energies of the homogeneous phases on either side of the interface, according to

$$\frac{NF_{i=polymer}}{\rho_0 k_B TV} = \phi_p \ln\phi_p + \frac{\chi_{ps}N}{2}\phi_s\phi_p + \frac{\chi_{pp}N}{2}\phi_p\phi_p \tag{16}$$

$$\frac{NF_{i=solvent}}{\rho_0 k_B TV} = \frac{\phi_s}{\alpha}\ln\left(\frac{\phi_s}{\alpha}\right) + \frac{\chi_{ps}N}{2}\phi_s\phi_p + \frac{\chi_{ss}N}{2}\phi_s\phi_s \tag{17}$$

$$\frac{NF_{i=holes}}{\rho_0 k_B TV} = \frac{\phi_h}{\alpha}\ln\left(\frac{\phi_h}{\alpha}\right) \tag{18}$$

In (16)-(18), the volume fractions ϕ_p, ϕ_s and ϕ_h should be taken as the bulk homogeneous volume fractions on either side of the interface according to

$$\phi_i^{(1)} = \varphi_i(z=0) \tag{19}$$

$$\phi_i^{(2)} = \varphi_i(z=L) \tag{20}$$

assuming a one-dimensional system with coordinate z, rather than as the overall volume fractions of the system. The construction (15) assumes the total system volume V can be split into two according to

$$V = V_1 + V_2 \tag{21}$$

where V_1 and V_2 are the volumes associated with two separate homogeneous systems with volume fractions of the various species equal to the bulk values on either side of the interface. Since V is known, V_1 and V_2 are not independent, and it suffices to know V_1, or rather the ratio V_1/V, in order to find the separated free energy F_s in (15). The interface calculated using SCFT is actually three superposed contributions due to the three species in the present system. Thus three different volume ratios V_1/V can be found which correspond to the interface of the polymer with the other two species, the interface of the solvent with the other two species, and the interface of the holes with the other two species. These ratios are then written as

$$\frac{V_{1i}}{V} = \frac{\phi_i^{(2)} - \phi_i}{\phi_i^{(2)} - \phi_i^{(1)}} \tag{22}$$

where $i = p, s$ or h, for the polymer, solvent or hole interfaces. A derivation of (22) is given by Matsen [30] for the case of a binary interface in terms of conservation considerations. The derivation is exactly the same in the present case.

With the expression (14) for the surface tension now defined, one can also break this expression up into its component parts in order to facilitate analysis of the results. The free energy (1) can be written as $F = U\text{-}TS$ or

$$\frac{NF}{\rho_0 k_B TV} = \frac{NU}{\rho_0 k_B TV} - \frac{NS}{\rho_0 k_B V} \quad . \tag{23}$$

Following Matsen and Bates [38], the free energy components would then be

$$\frac{NU_{ps}}{\rho_0 k_B TV} = \frac{\chi_{ps} N}{V} \int d\mathbf{r} \varphi_p(\mathbf{r}) \varphi_s(\mathbf{r}) \tag{24}$$

$$\frac{NU_{ss}}{\rho_0 k_B TV} = \frac{\chi_{ss} N}{2V} \int d\mathbf{r} \varphi_s(\mathbf{r}) \varphi_s(\mathbf{r}) \tag{25}$$

$$\frac{NU_{pp}}{\rho_0 k_B TV} = \frac{\chi_{pp} N}{2V} \int d\mathbf{r} \varphi_p(\mathbf{r}) \varphi_p(\mathbf{r}) \tag{26}$$

$$\frac{-S_{Tp}}{\rho_0 k_B V} = \frac{1}{V} \int d\mathbf{r} \rho_p \ln \rho_p \tag{27}$$

$$\frac{-S_{Cp}}{\rho_0 k_B V} = \frac{1}{V} \int d\mathbf{r} \rho_p \ln q(\mathbf{r},1) \tag{28}$$

$$\frac{-S_{Ts}}{\rho_0 k_B V} = -\frac{\phi_s}{\alpha} \ln\left(\frac{Q_s \alpha}{\phi_s V}\right) - \frac{1}{V} \int d\mathbf{r} \omega_s(\mathbf{r}) \varphi_s(\mathbf{r}) \tag{29}$$

$$\frac{-S_{Th}}{\rho_0 k_B V} = -\frac{\phi_h}{\alpha} \ln\left(\frac{Q_h \alpha}{\phi_h V}\right) - \frac{1}{V} \int d\mathbf{r} \omega_h(\mathbf{r}) \varphi_h(\mathbf{r}) \tag{30}$$

for the internal energy contribution to the free energy between polymer segment and solvent, solvent and solvent, polymer and polymer, translational entropy contribution to the free energy of the polymer, configurational entropy of the polymer, translational entropy of the solvent and the translational entropy of the holes, respectively. The configurational entropy accounts for all the different conformations a polymer can take, whereas the translational entropy of the polymer accounts for the remaining positional degrees of freedom of the center of mass of a molecule. In (27) and (29), ϱ_p is defined as

$$\rho_p \equiv \frac{\phi_p V q(\mathbf{r},1)}{Q_p} \tag{31}$$

The components (24)-(30) can be converted into excess free energy components by subtracting off the corresponding bulk free energy components of the homogeneous phases on either side of the interface in exactly the same way as for the total free energy. Then by dividing by the interfacial area, these can be converted into components of the surface tension, just as the total excess free energy was expressed as a surface tension. These internal energy and entropic contributions to the surface tension will be used to explain the trends observed experimentally and theoretically in the supercritical carbon dioxide-polystyrene system.

Results and Discussion

Surface tension as a function of temperature and pressure

A typical pendant drop image is shown in Figure 1. The surface tension of polystyrene melt in carbon dioxide was measured at five different pressures: 500, 1000, 1500, 2000, and 2500 psi, and five different temperatures: 170, 180, 190, 200, and 210°C. Figure 2 shows the surface

tension values as a function of time. The average of the surface tension values is taken as the equilibrium surface tension when the change in surface tension is less than 0.0001mJ $m^{-2}s^{-1}$ for 1 hour. Errors are on the order of 0.01 mJ m^{-2}. All measurements show that the surface tension reaches its equilibrium value quickly, within 15 minutes. The surface tension values from these experiments show trends of being smaller at higher temperatures and higher pressures, consistent with the data from other studies [24].

From Fig. 2, equilibrium surface tension values of polystyrene in carbon dioxide under various conditions can be obtained by averaging the plateau data points at each condition; the results are shown in Fig. 3. It is apparent that the dependence of surface tension on temperature becomes less with increasing pressure. When the pressure value reaches above ~ 2000 psi, such dependence becomes nil. This implies that increasing temperature is effective at reducing surface tension only when moderate pressure is applied during a polymer process.

To find how temperature and pressure influence the surface tension, a 2nd order linear regression model is used [39]. Table 1 shows ANOVA (analysis of variance), indicating the validity of the regression model: the observed F-value is larger than the tabulated F-value at the 95% confidence level. In Table 2, the validity of each parameter was also examined using a t-test: all observed t values are greater than the tabulated t-value at the 95% confidence level. From these statistical investigations, we can propose the following equation

$$\gamma = 38.7032 - 0.0559\,T - 0.0100\,P + (2.596\text{X}10^{-5})TP \qquad (32)$$

$$(170\ ^{o}\text{C} \le T \le 210^{o}\text{C},\ 500\ \text{psi} \le P \le 2500\ \text{psi})$$

where the surface tension of polystyrene in supercritical CO_2 γ is in [mJ/m^2], the temperature T in [°C], and the pressure P in [psi]. Note that the second order terms in T and P are absent; statistically, γ is linearly related to T and P. However, there is an interaction term in (TP),

indicating γ dependence on T or P is affected by P or T, respectively. This indicates that, for polymer melt processes, one has to adjust both T and P in order to control the value of γ completely.

From (32), the following equations can be derived:

$$\frac{\partial \gamma}{\partial T} = -0.0559 + (2.596X10^{-5})P \tag{33}$$

$$\frac{\partial \gamma}{\partial P} = -0.0100 + (2.596X10^{-5})T \tag{34}$$

$$\frac{\partial^2 \gamma}{\partial P \partial T} = 2.596X10^{-5} \tag{35}$$

There are three main experimental trends presented in Eqs. (33-35). These are the dropping of surface tension as a function of temperature for the pressure being less than ~ 2153 psi, the dropping of surface tension with increasing pressure for the temperature being less than ~ 385°C, and the flattening of the surface tension versus temperature curves with increased pressure (see also Figure 3). When the pressure is greater than 2153 psi or the temperature is greater than 385°C, these trends become trivial, which hence defines the validity limits of the above statements and, maybe, the empirical equations.

Self-consistent field theory was used to explain the aforementioned trends. SCFT calculations have been performed to find a dimensionless surface tension $(R_g\gamma / a^2\rho_0 k_B T)$ as described in the Theory section, as a function of temperature at two different pressures. The results are shown in Figure 4. For the high pressure run, no holes were included and the overall volume fractions were taken as ϕ_p=0.65 and ϕ_s=0.35 for the polymer and solvent, respectively. This corresponds to an incompressible fluid, and thus is the highest pressure case possible. This was compared

against a lower pressure run with ϕ_p =0.60 and ϕ_s =0.30, or in other words, with 10 percent holes by volume. In both cases and at all temperatures, the system size was L=12.0R_g. The ratio α of the volume of a solvent molecule to that of a polymer molecule was taken to be 0.1 for both pressure runs. This is not particularly realistic, as this ratio for the supercritical carbon dioxide-polystyrene system should be a much smaller number. Too great a size disparity between the different molecular species will however cause numerical difficulties. This results from the extremely high translational entropy that results from having many, very small solvent molecules. This strongly favours mixing, and makes it difficult to establish an interface unless the Flory-Huggins parameters are turned up extremely high. This in turn makes it difficult to achieve numerical accuracy in the calculations. Rather, we will take a qualitative approach, making sure that trends observed experimentally are nonetheless still observed in the calculations despite a large value for α. The mechanisms found to be responsible for the three aforementioned experimental trends should still be valid for more disparate molecular sizes. For this reason, we have not changed the hole volume fractions into pressure values through osmotic pressure calculations, as was previously mentioned to be possible.

The parameters left to specify now are the Flory-Huggins values. Since a qualitative philosophy is being used, our model system need not incorporate χ values determined from first principles or from further experimentation. Rather, it suffices to choose values that map our model system qualitatively onto the experimental structure. A relationship between χ (or in this case, χN) and temperature T that is commonly used is [40, 41]

$$\chi N = \frac{A}{T} + B \qquad (36)$$

where A and B are constants. In the present work, we have three different such parameters, namely $\chi_{ps}N$, $\chi_{ss}N$ and, $\chi_{pp}N$, so we will have three sets of constants, A_{ps}, B_{ps}, A_{ss}, B_{ss} and A_{pp}, B_{pp}. Since we are looking for qualitative trends, we are free to set B_{ps}, B_{ss} and B_{pp} all equal to zero, for simplicity. The most basic model system that we could devise that still produced a structure of the interface that would qualitatively resemble the experimental system involved setting A_{pp}=0. From (36), this can only be satisfied for arbitrary T if $\chi_{pp}N$ =0, always. We tried runs with different values of A_{pp} but found no qualitative differences. Lastly, we will choose A_{ps}=100 and A_{ss}=150. This way, we can range T, in arbitrary units, from 2.0 to 2.5 and get

$$2.0 < T < 2.5$$

$$50 > \chi_{ps}N > 40$$

$$75 > \chi_{ss}N > 60.$$

These values produce reasonable interfacial structures, as shown in Figure 5 for T=2.0 and T=2.5 at the two different pressures. To assign specific units to the temperature such as Kelvin or degrees centigrade, the parameters A should be specified in the desired units. The present values were chosen so as to reproduce an appropriate interface while at the same time allowing for numerically accurate calculations.

Temperature dependence

We may now return to Figure 4 and explain the three main trends previously mentioned. The temperature dependence of our model system can be seen to follow the trends of experiment

and the empirical equation (32) at both pressures in that surface tension decreases with increasing temperature. In Figure 6 the components of the surface tension which were described in the theory section are plotted [42]. The two main components that can be seen to be contributing to the decrease of surface tension with temperature are the internal energy contribution to the surface tension (open circles on solid curve) and the polymer configurational entropy contribution to the surface tension (crossed dotted curve), see also Table 3, rows m_l and m_h. The translational entropy of the holes contributes negligibly. Of these, the largest contribution is from the internal energy. This contribution can in turn be split into the polymer-solvent, solvent-solvent, and polymer-polymer components of the internal energy contribution to the surface tension, as shown in Figure 7. In that figure, the component that is clearly responsible for the overall drop of the total internal energy contribution is the polymer-solvent component; it is the only component with a slope in the correct direction. Translating this conclusion into polymer-solvent processes, one would concentrate on modifying the molecular interaction between the polymer and its solvent when making use of such temperature dependence of surface tension. Under this situation, modifications of polymer or solvent molecular properties alone could be less effective at reducing surface tension with an elevated temperature.

That the polymer-solvent internal energy contribution is responsible for the drop in surface tension makes perfect sense, in that the free energy of the system can be split according to equation (23) into an internal energy part and an entropic part, the two parts having different signs, that is, they oppose each other. The entropic contributions promote mixing whereas the internal energy favours segregation [43]. As the temperature is increased, the $\chi_{ps}N$ parameter decreases, reducing the segregation between polymer and solvent segments. This means the entropy becomes a larger relative portion of the free energy, more mixing takes place and the

interface becomes more diffuse; this in turn means there will be a lower surface tension. This is a well known and understood effect which is correctly reproduced here in the model system.

Pressure dependence

In Figure 4 it can be seen that the surface tension versus temperature curve drops to lower surface tension for a higher pressure. This is again in agreement with the experimental findings and empirical equation (32). The components of the surface tension that drop are the internal energy, the configurational entropy of the polymer and the translational entropy of the solvent; this can be seen from Figure 6 by comparing panels (a) and (b) or by examining Table 5, rows value $_{l}$ and value $_{h}$. Again, the largest single factor causing this drop is the internal energy contribution. In Figure 7, however, we see that for the pressure induced tension drop, the responsible sub-component is not the polymer-solvent internal energy as for the temperature case, but rather the solvent-solvent sub-component. Translating this conclusion into industrial polymer-solvent processes, one could simply focus on modifying the molecular self-interaction among solvent molecules when making use of such pressure dependence of surface tension.

The above conclusion can be understood in terms of a reduction of dilution by the holes. At higher pressure, there are fewer holes present. Since $\chi_{ss}N$ has been chosen to be positive, solvent molecules prefer to be in an environment of holes rather than in an environment of other solvent molecules; in the former situation the unfavourable solvent-solvent contact energy is diluted by the holes. With the removal of holes at higher pressure, this dilution is reduced, the solvent-solvent contact energy goes up, and so does the free energy. This effect takes place predominantly in the bulk solvent side of the interface where the majority of solvent molecules

can be found. This means the bulk free energy $F_h^{(1)}$ appearing in equation (15) and thus in (14) is increased. This increased quantity is subtracted off the total free energy (1) to find the surface tension, therefore the surface tension will drop [44].

This last point may be understood in terms of density. The removal of holes is the same as an increase in density in the region where the holes are being removed. Thus the surface tension drops when the solvent phase increases in density to be more similar to the density on the polymer side of the interface. Thus one can say the drop in surface tension with increasing pressure is due to a reduction of the density difference between two sides of the interface.

The above analysis of pressure dependence requires a χ_{ss} that is positive, and so it is appropriate here to discuss what might be the case if χ_{ss} were negative. This is important since from the first principles definition of χ_{ss} given in equation (2) one would expect that χ_{ss} would normally be less than zero, that is, the solvent molecules would have some slight attraction. For more realistic choices of α, the translational entropy of the solvent would not be negligible. Therefore instead of holes diluting the solvent phase for energetic reasons, the holes would dilute the phase for entropic reasons. The explanation would remain the same for the pressure dependence beyond this, and the density difference interpretation would still hold. As α is increased, the translational entropy of the solvent will become less important, and to maintain the interface structure, χ_{ss} must be made less negative. For a very large α, such as is being used here, χ_{ss} must become positive to draw the hole molecules into the solvent phase to reproduce the experimental configuration. At this point, χ_{ss} must be viewed entirely as a phenomenological parameter.

Change in temperature dependence with pressure

In addition to an overall drop in surface tension upon increasing pressure, the temperature dependence of the surface tension is less pronounced at high pressures than at lower pressures. This is seen in Figure 4 where the dotted curve is a repetition of the high pressure curve (dashed) shifted upwards to lie on top of the lower pressure curve (solid). One can clearly see the shallower slope with temperature of the high pressure results. This is again in agreement with the experimental findings and the empirical equation (32).

From Figure 6, one can compute linear slopes for all the components of the surface tensions in order to find which components are responsible for this reduction in steepness. Table 3, row Δm shows the difference between the component slopes. It is found that the translational entropy components of the polymer, solvent and holes all contribute to the overall reduction in steepness. The hole contribution is negligible compared to the other two and can safely be ignored. Thus it is the polymer and solvent translational entropy contributions to the surface tensions that cause the shallowness of the high pressure results.

This can be explained in terms of the presence or absence of holes. The presence of holes can only affect the system in two ways: through energy dilution as discussed in the pressure dependence subsection, or through adding translational entropy. The latter has already been said to be insignificant, and so we are left with energy dilution alone. At low pressures, the solvent-solvent contacts are diluted by the holes, reducing the system free energy. At high pressures, solvent-solvent contacts cannot be reduced by holes anymore, so the only possibility for reducing these contacts is for the solvent to be near polymer segments. This induces increased mixing, and thus increased translational entropy of both the solvent and the polymer. This increased mixing partially counteracts the internal energy segregation effect that is a function of temperature. Thus

the surface tension profile with temperature is flatter at higher pressures than at lower pressures where this polymer-solvent mixing is unnecessary due to the presence of the holes. In other words, when the solvent is at higher density, there is a greater mixing effect that counteracts the formation of an interface due to a solvent-solvent internal energy reduction upon absorbing solvent into the polymer phase.

For small α values and negative χ_{ss} parameters, the same mechanism is expected to function, except that translational entropy will force the holes into the solvent phase rather than energetic considerations, along the lines explained in the pressure dependence section.

Simple liquid models

In all three aforementioned trends, theory was able to reproduce and explain the experimental results. The explanations did not require any consideration of the configurational entropy contribution to the surface tension. This then could explain why simple liquid theory models of polymer interfaces such as those discussed by Dee and Sauer [16] or Jones and Richards [17] can be quantitatively reliable. We anticipate that the configurational entropy contributions would become even less significant for lower α values, that is, for more realistic volume ratios between the solvent and polymer. Preliminary runs with smaller values of α (not included) seem to bear this out. Upon reducing α, the number of solvent molecules must increase in order to preserve the same overall volume fraction of solvent. This increases the translational entropy component of the solvent, and weakens the interface. To have a stable interface for very small α, one must counteract this by greatly increasing the segregations. This will increase the internal energy contribution relative to the configurational entropy of the polymer for a similar width of interface. Thus if the model were to be made more realistic, the configurational entropy would

become less important, further justifying the use of simple liquid models. Specifically, if the configurational entropy of the polymer to the surface tension was to be subtracted out of the results, the same qualitative results would be found. This is not true of the other quantitatively significant contributions to the surface tension, see Figure 6. Therefore, one can say that the theoretical explanations of the experimental results may not require any consideration of the configuational entropy contribution to the surface tension. In fact, if gradient terms are kept in the SCFT description of the polymer system along the lines of Hong and Noolandi [34], then upon ignoring configurational degrees of freedom of the polymer in the SCFT formalism, one might expect to arrive at a theory very similar to density gradient theory (square density theory, Cahn-Hilliard theory). Theories of this sort have been shown to give very good quantitative agreement [45], although being phenomenological, they cannot explain the microscopic origins of the trends they predict. It is precisely this explanatory feature of SCFT that motivates its present use.

Summary

A comprehensive set of the surface tension data of polystyrene in supercritical carbon dioxide at various temperatures and pressures was obtained successfully. Based on the obtained data, an empirical equation was developed that predicts the surface tension value at a given temperature and pressure. Within the experimental limits on temperature (< ~385°C) and pressure (< ~2153 psi), the trends of surface tension dependence on temperature and pressure can be quantified with partial derivatives of the empirical equation.

Self-consistent field theory calculations were performed on a model system and surface tension trends involving temperature, pressure, and temperature with pressure were explained in the terms of the components of the surface tension. In particular, the reduction of surface tension with increasing temperature was consistent with a reduction of segregation between the molecular constituents; the reduction of surface tension with increasing pressure was due to increased similarity of density between the polymer (polystyrene) and solvent (supercritical carbon dioxide) constituents; the flattening of the surface tension versus temperature curve with increasing pressure was due to extra mixing between polymer and solvent, which reduces the segregation of the species at high pressures. The extra mixing results from the similar densities of the molecules at high pressures. None of these findings were dependent on the configurational entropy contribution of the polymers to the surface tensions, and so the use of simple liquid models for the prediction of surface tensions is justified. Consideration should be given to the above mechanisms when attempting to engineer surface tension properties.

Acknowledgements

We gratefully acknowledge the financial support from the Natural Sciences and Engineering Research Council of Canada (NSERC), Canadian Foundation for Innovation (CFI) and the Canada Research Chairs (CRC) Program.

References

1. Myers, D., Surfaces, Interfaces, and Colloids: Principles and Applications; VCH publishers Inc: New York, 1991.

2. Cahn, J. W.; Hilliard J. E. J. Chem. Phys. **1959**, 31, 688-699.

3. Goel, S. K.; Beckman, E. J. Polym. Eng. Sci. **1994**, 34, 1137-1147.

4. Russell, K. N. Adv. Colloids Interf. Sci. **1980**, 13, 205-318.

5. Colton, J. S.; Suh, N. P. Polym. Eng. Sci. **1987,** 27, 500-503.

6. del Rio, O. I.; Neumann, A.W. J. Colloid Interface Sci. **1997**, 196, 136-147.

7. Rotenberg, Y.; Boruvka, L., Neumann, A. W. J. Colloid Interface Sci. **1983,** 93, 169-183.

8. Song, B.; Springer, J., J. Colloid Interface Sci. **1996**, 184, 77-91.

9. Anastasiadis, S. H.; Chen, J. K.; Koberstein, J. T.; Sohn, J. E.; Emerson, J. A. Polym. Eng. Sci. **1986**, 26, 1410-1428.

10. Demarquette, N. R.; Kamal, M. R. Polym. Eng. Sci. **1994**, 34, 1823-1833.

11. Kwok, D. Y.; Cheung, L. K.; Park, C. B.; Neumann, A. W. Polym. Eng. Sci. **1998**, 38, 757-764.

12. Wu, S. J. Phys. Chem. **1970**,74, 632-638.

13. Cooper, A. I. J. Mat. Chem. **2000**, 10, 207-234.

14. Tomasko, D. L.; Li, H; Liu, D.; Han, X.; Wingert, M. J.; Lee, L. J.; Koelling K. W Ind. Eng. Chem. Res. **2003**, 42, 6431-6456.

15. Lee, M.; Park, C. B.; Tzoganakis, C., Polym. Eng. Sci., **1999**, 39, 99-109.

16. Dee, G. T.; Sauer, B. B. Adv. Phys. **1998**, 47, 161-205.

17. Jones, R. A. L.; Richards, R. W., Polymers at Surfaces and Interfaces; Cambridge University Press: New York, 1999.

18. Park, H.; Park, C. B.; Tzoganakis, C.; Tan, K. H.; Chen, P Ind. Eng. Chem. Res. **2006**, 45, 1650-1658.

19. Cheng, P.; Li, D.; Boruvka, L.; Rotenberg Y.; Newmann, A.W. Colloids and Surfaces, **1990**, 43, 151-167.

20. Susnar, S. S.; Hamza H.A.; Newmann, A.W. Colloids and Surfaces, **1994**, 89, 169-180.

21. Andreans, J. M.; Hauser, E.A.; Trucker W.B. J. Phy.Chem.**1938**, 42, 1001-1019.

22. Cheng, P.; Neumann, A. W. Colloids and Surfaces, 1**992**, 62, 297-305.

23. Xue, A; Tzoganakis, C.; Chen, P. Polym. Eng. Sci. **2004**, 44, 18-27.

24. Li, H.; Lee, L. J.; Tomasko, D. L. Ind. Eng. Chem. Res**. 2004**, 43, 509-514.

25. Funami, E.; Taki, K.; Murakami T.; Kihara S., Polymer Processing Society Annual Meeting, **2006**, Paper No. SP2.18

26. Sanchez I. C.; Lacombe R. H. Macromolecules **1978**, 11, 1145-1156.

27. Sanchez, I. C.; Lacombe R. H. J. Phys. Chem. **1976**, 80, 2352-2363.

28. Sato, Y.; Takikawa, T.; Takishima, S.; Masuoka, H. J. of Supercritical Fluids **2001**, 19, 187-198.

29. Li, G.; Wang, J., Park, C. B.; Moulinie, P,; Shimha, R.,Annu. Tech. Conf.-Soc. Plast. Eng., **2004**, Paper No.421.

30. Matsen M. W. In Soft Matter Volume 1; Eds. Gompper, G; Schick, M.; Wiley-VCH :Weinheim, **2005,** 87-178.

31. Matsen, M. W. J. Phys. Condens. Matter **2002,** 14, R21-R47.

32. Fredrickson, G. H.; Ganesan, V.; Drolet, F. Macromolecules **2002,** 35, 16-39.

33. Schmid, F. J. Phys. Condens. Matter **1998**, 10, 8105-8138.

34. Hong , K. M.; Noolandi, J. Macromolecules **1981**, 14, 1229-1234.

35. Binder, K.; Müller, M.; Virnau, P.; MacDowell, L.G. Adv. Polym. Sci. **2005**, 173, 1-110.

36. $\chi_{ps}, \chi_{ph}, \chi_{sh}$ could equally be used instead of $\chi_{ps}, \chi_{pp}, \chi_{ss}$. This would not change any of the results .

37. Thompson, R. B.; Rasmussen, K. Ø.; Lookman, T., J. Chem. Phys., **2004**, 120, 31-34.

38. Matsen, M.W.; Bates, F. S. J. Chem. Phys. **1997,** 106, 2436-2448.

39. Milton, J. S.; Arnold, J. C. Introduction to probability and statistics; McGraw-Hill Inc.: New York, 1995.

40. Mai , S.-M.; Fairclough, J. P. A.; Terrill, N. J.; Turner, S. C.; Hamley, I. W.; Matsen, M. W.; Ryan, A. J.; Booth, C. Macromolecules **1998**, 31, 8110-8116.

41. Mai, S. -M.; Mingvanish W.; Turner S. C.; Chaibundit, C.; J. P. A.; Heatley, F.; Matsen, M. W.; Ryan, A. J.; Booth C. Macromolecules **2000,** 33, 5124-5130.

42. The total surface tension must of course be a positive value, the zero being the absence of any interface. The components however can be either positive or negative.

43. The configurational entropy contribution of the polymer to the surface tension is the only entropic contribution that has positive values. This comes about because the conformations are restricted at the interface compared to the bulk.

44. The total free energy will also increase upon the removal of holes, but since the dilution is taking place predominantly in the solvent bulk region, the total free energy will increase less than the bulk free energy of the solvent side of the interface. Thus the interfacial tension will still drop.

45. Enders, S.; Kahl, H.; Winkelmann, Fluid Phase Equilibria, **2005**, 228-229, 511-522.

Key Words

Surface Tension, Supercritical Carbon Dioxide, Polystyrene, Excess Entropy, Axisymmetric Drop Shape Analysis (ADSA), Entropy, Self-consistent field theory, Sanchez-Lacombe equation of state

Table 1. ANOVA (analysis of variance) table for a 2nd order linear regression model

	Sum of Square (SS)	Degree of Freedom	Mean Square(MS)
Regression	560.83	3	180.95
Residual	7.62	46	0.165
Total	568.45	49	
F_{obs}=1129.9 $F_{3,46,0.05}$=2.80, R^2=0.999			

Table 2. t-test for evaluating each parameter of the proposed 2nd order linear regression

$\gamma = 38.7032 - 0.0559\,T - 0.0100\,P + (2.596\text{X}10^{-5})TP$

$(170\ ^{o}\text{C} \le T \le 210^{o}\text{C},\ 500\ \text{psi} \le P \le 2500\ \text{psi})$

Parameters	Coefficients	Standard Error	$\lvert T_{obs} \rvert$
Intercept	38.7032	2.0083	19.27
Temperature(T)	-0.0559	0.0105	5.30
Pressure(P)	-0.0200	0.0012	8.52
Pressure^2(P^2)	2.5957E-05	6.13E-08	4.23
$T_{0.025,46}$=2.013			

Table 3. Slopes of the components of the surface tension from figure 6 assuming linearity. Contributions of the various components are labeled without including multiplicative factors. ml refers to the slope of the low pressure run and mh to the high pressure run. Units are inverse arbitrary temperature. Δm is the difference between the slopes of the low and high pressure runs. Value l and value h are midpoint values of the low and high pressure runs, respectively, taken from Figure 6.

	γ	U	S_{Tp}	S_{Cp}	S_{Ts}	S_{Th}
m_l	-1.05	-0.69	0	-0.45	0.12	-0.02
m_h	-0.72	-1.07	0.25	-0.49	0.59	0.00
Δm	0.33	-0.38	0.25	-0.04	0.47	0.02
value $_l$	0.97	2.22	-0.46	0.46	-0.95	-0.30
value $_h$	0.29	1.62	-0.42	0.23	-1.14	0.00

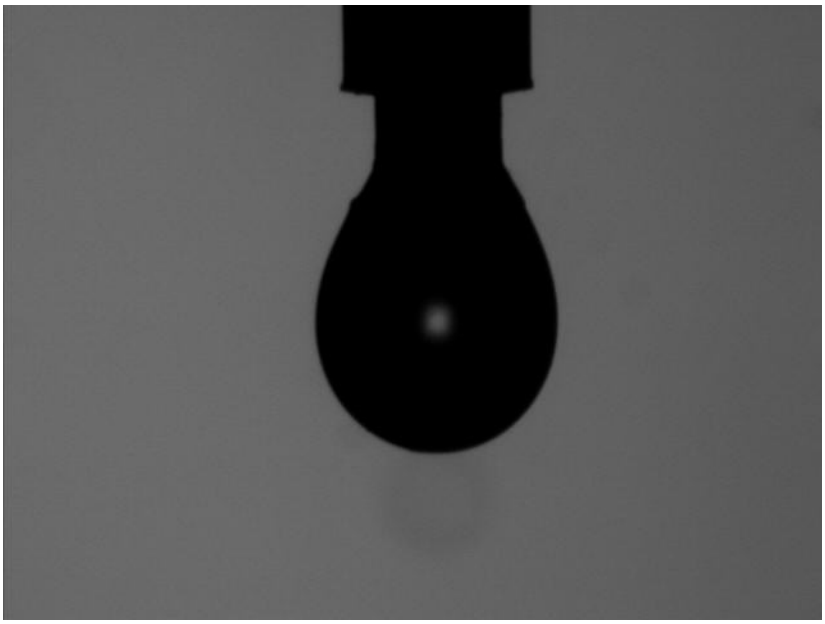

Figure 1. A typical pendant drop image of polystyrene in supercritical carbon dioxide

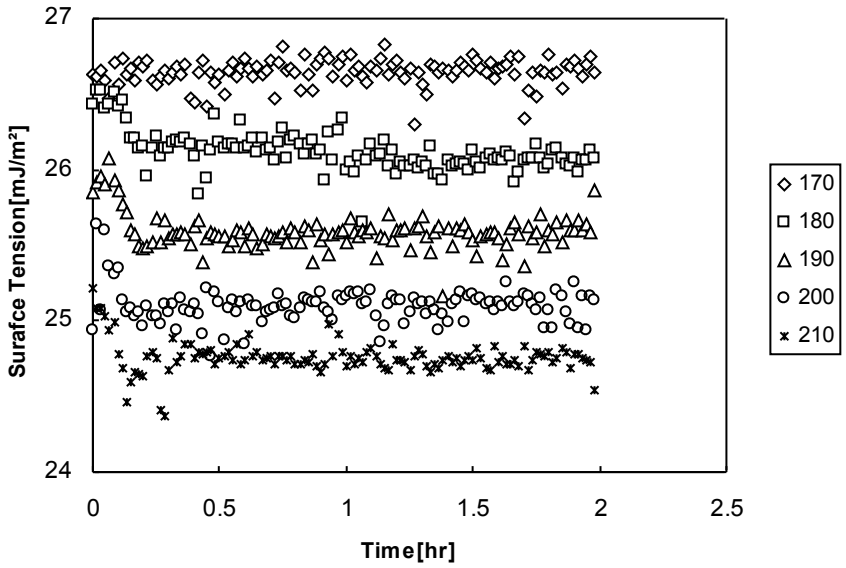

Figure 2. Surface tension of polystyrene in supercritical carbon dioxide at a pressure of 500psi..

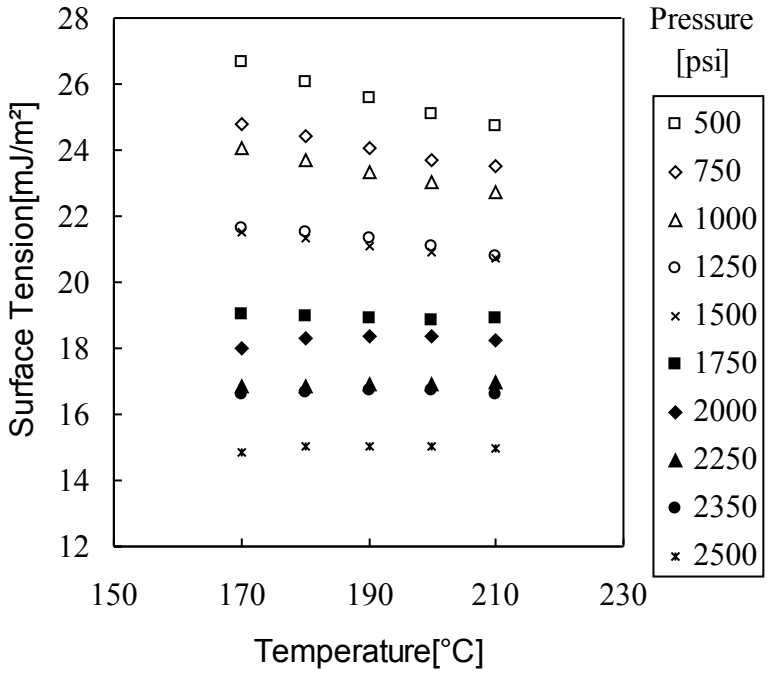

Figure 3. The equilibrium surface tension of polystyrene in carbon dioxide at various temperatures and pressures

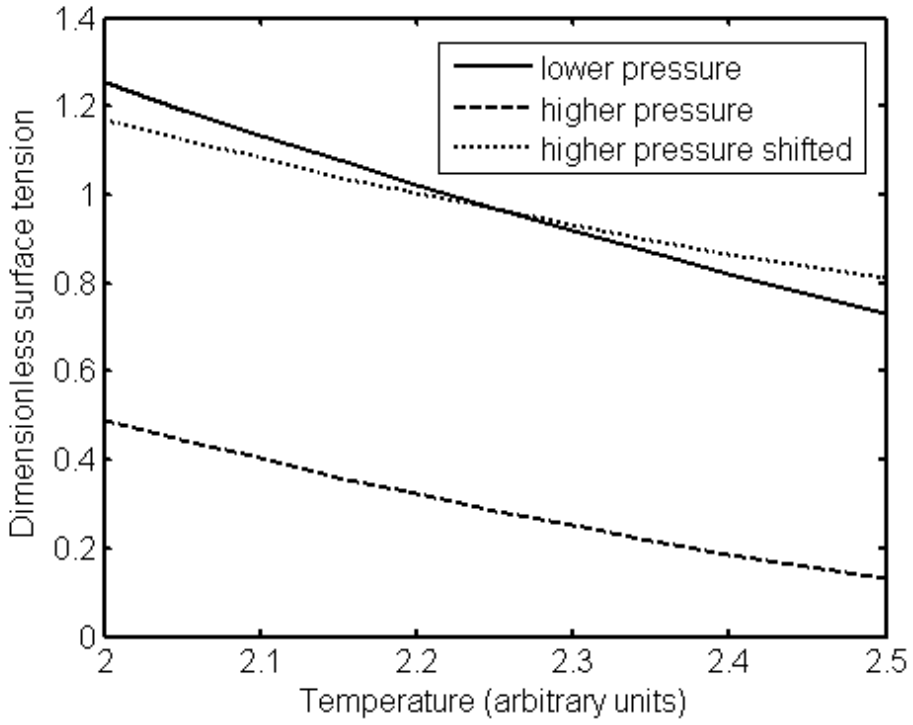

Figure 4. Dimensionless surface tension as a function of temperature for two different pressures. The lower pressure run is the solid curve while the higher pressure run is the dashed curve. The higher pressure run is also plotted a second time by a dotted curve where it is shifted upwards to more easily compare the slopes of the two runs.

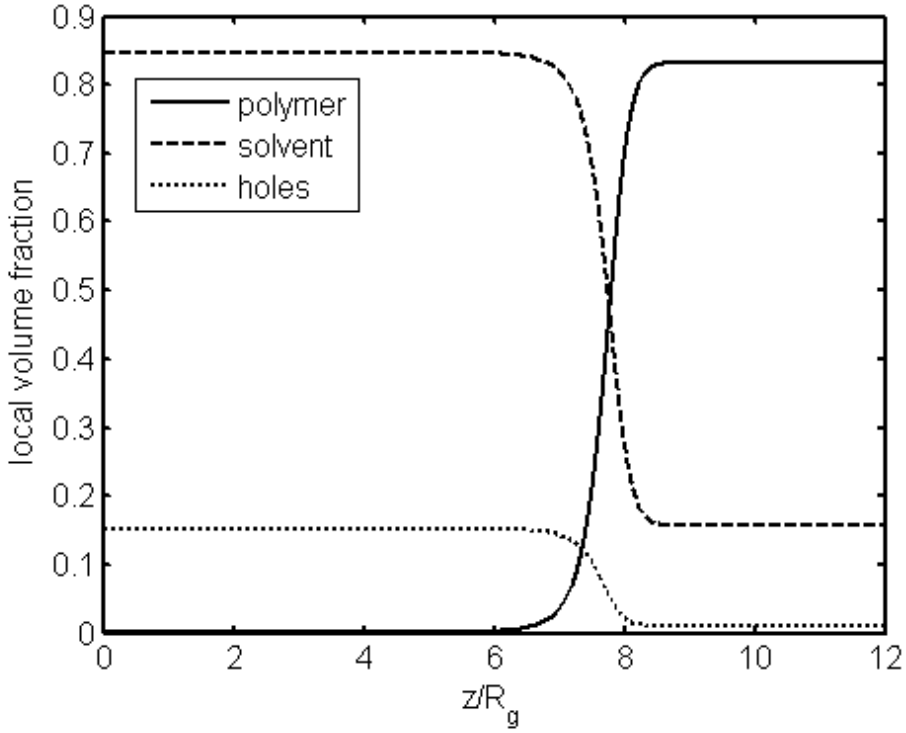
polymer
solvent
holes
local volume fraction
z/R_g
0
0.1
0.2
0.3
0.4
0.5
0.6
0.7
0.8
0.9
0
2
4
6
8
10
12

(a)

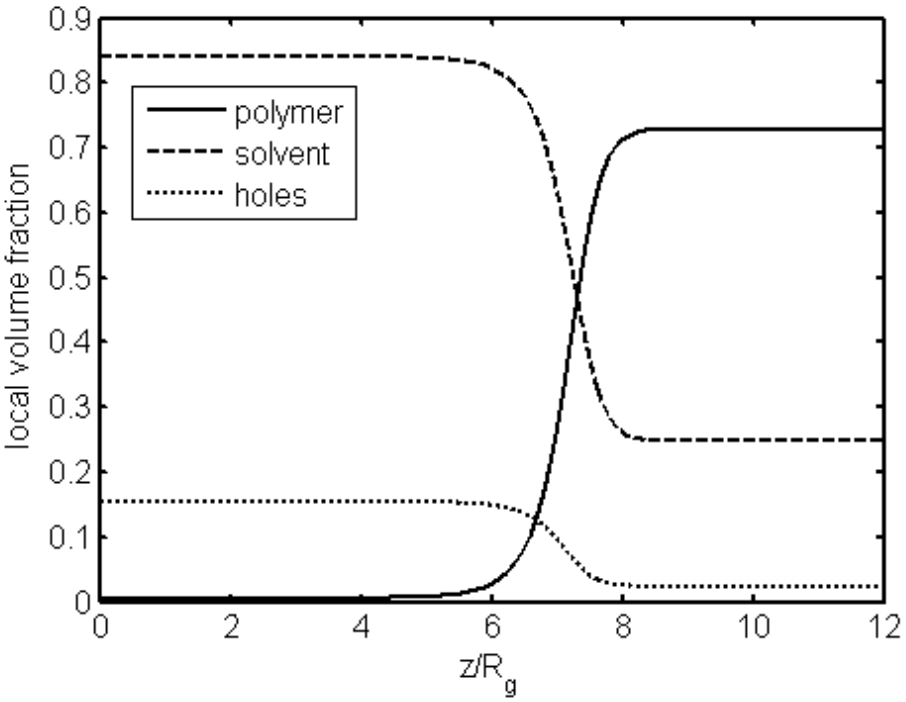
polymer
solvent
holes
local volume fraction
z/R_g
0
0.1
0.2
0.3
0.4
0.5
0.6
0.7
0.8
0.9
0
2
4
6
8
10
12

(b)

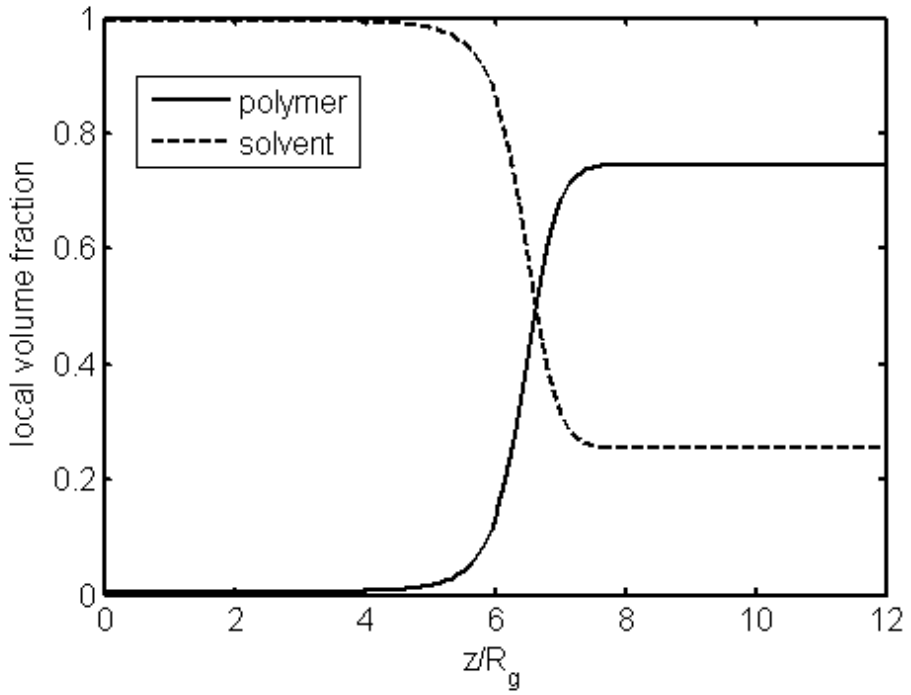
polymer
solvent
local volume fraction
z/R_g
0
0.2
0.4
0.6
0.8
1
0
2
4
6
8
10
12

(c)

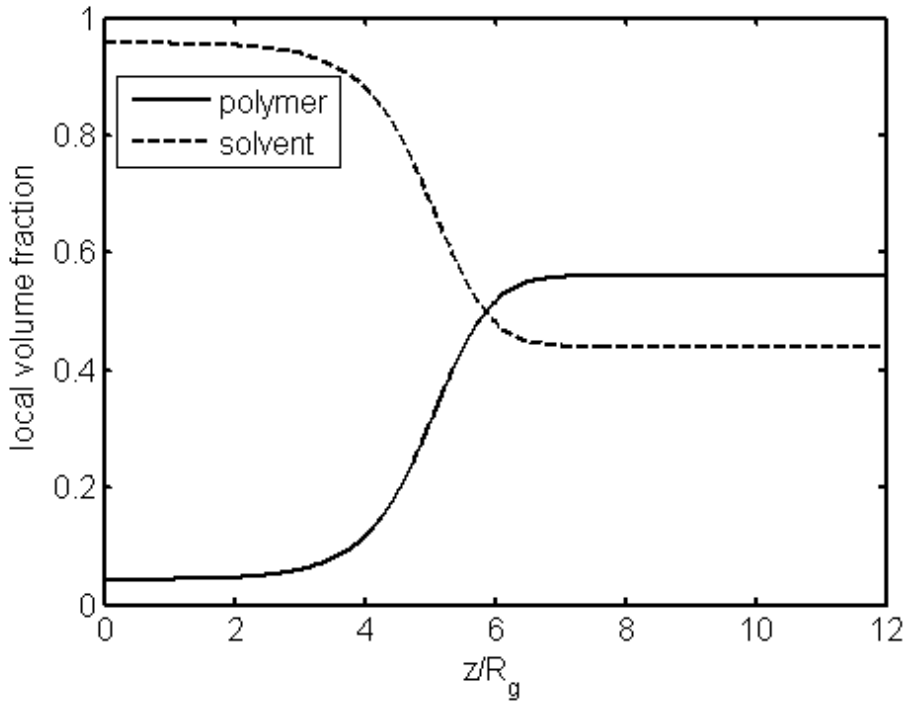

(d)

Figure 5 Concentration profiles for SCFT calculations. (a) Lower pressure, T=2.0. (b) Lower pressure, T=2.5. (c) Higher pressure, T=2.0. (d) Higher pressure, T=2.5.

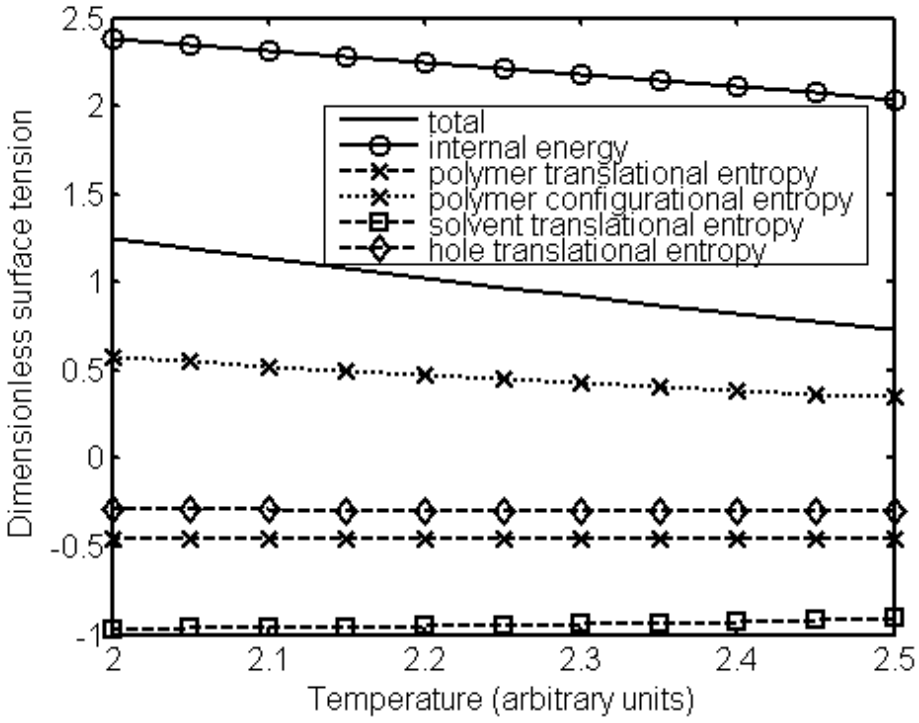
2.5
2
1.5
1
0.5
0
-0.5
-1
2
2.1
2.2
2.3
2.4
2.5
Dimensionless surface tension
Temperature (arbitrary units)
total
internal energy
polymer translational entropy
polymer configurational entropy
solvent translational entropy
hole translational entropy

(a)

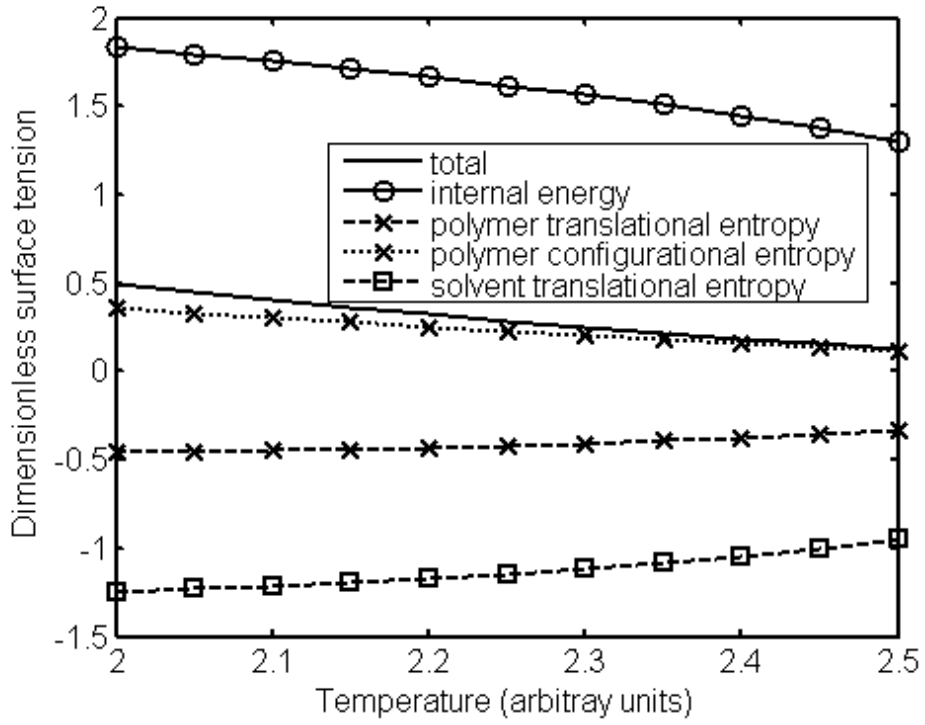

(b)

Figure 6 Components of the surface tension for (a) the lower pressure run and (b) the higher pressure run. Different contributions to the surface tension are shown in the legends.

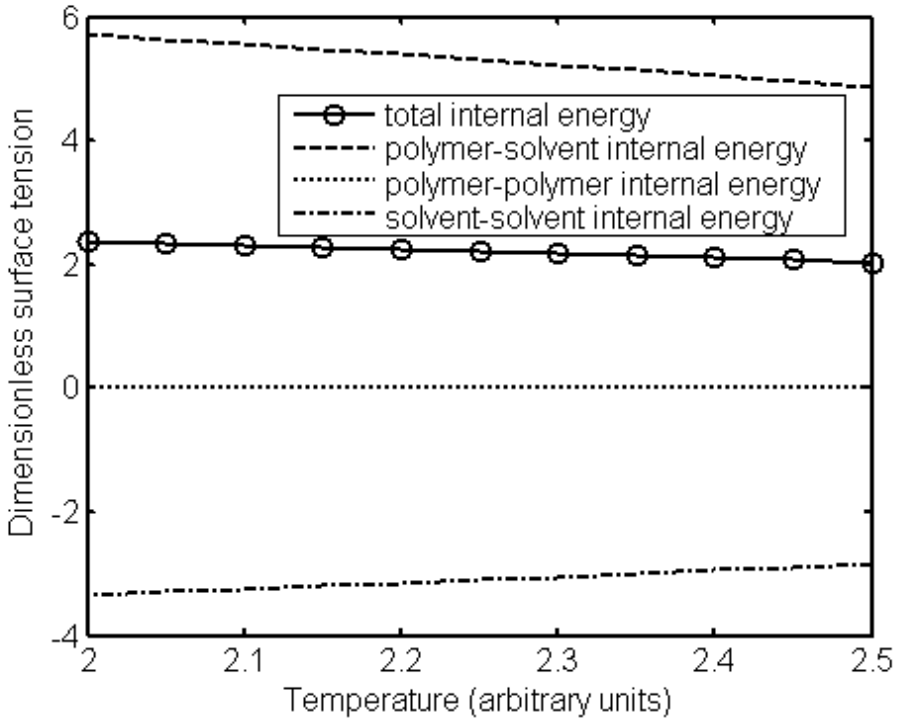
6
4
2
0
-2
-4
2
2.1
2.2
2.3
2.4
2.5
Dimensionless surface tension
Temperature (arbitrary units)
total internal energy
polymer-solvent internal energy
polymer-polymer internal energy
solvent-solvent internal energy

(a)

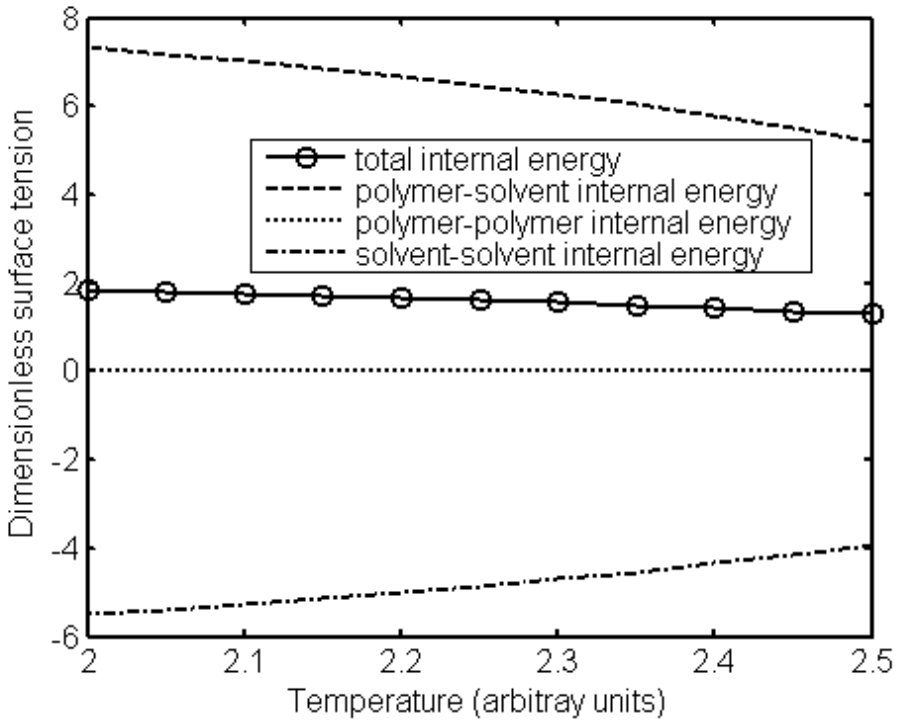

(b)

Figure 7. Sub-components of the internal energy contribution to the surface tension for the (a) lower pressure run and (b) the higher pressure run. Different contributions to the surface tension are shown in the legends.